Pure & Appl. Chem., Vol. 49, pp. 915 - 928. Pergamon Press, 1977. Printed in Great Britain.

RECENT STUDIES OF LIGHT SCATTERING FROM POLYMER FILMS*

Richard S. Stein$^{\phi}$, A. Misra^{+}, T. Yuasa† & F. Khambatta^{o}

Polymer Research Institute & Department of Chemistry, University of Massachusetts, Amherst, MA 01002, U.S.A.

Abstract - Experimental procedures for studying the scattering of light from polymer films are reviewed. The theory for scattering from spherulites is described and procedures for correction for multiple scattering, truncation, and disorder are described and illustrated for studies on polyethylene terephthalate films. Means for following crystallization kinetics from quantitative measurements of scattered intensities are outlined.

INTRODUCTION

The use of light scattering for the study of the structure of crystalline polymer films is now approximately twenty years old[1,2]. The earlier work[3,4], based upon the use of the Debye-Bueche[5] theory for the scattering from materials possessing random density fluctuations, was supplemented by model calculations for representing the scattering by spherulitic structures[1]. In these calculations, the scattering from an array of spherulites (Fig. 1) (composed of spherically symmetrical aggregates of polymer crystals and amorphous chains) was idealized as an anisotropic sphere of radius R_s having radial and tangential polarizabilities α_r and α_t immersed in an isotropic matrix with polarizability α_s. This leads to the equations

$$R_{H_v} = \frac{16\pi^4}{\lambda_o^4}\left(\frac{4}{3}\pi R_s^3\right)^2 \cos^2\rho_2\,(\alpha_r - \alpha_t)^2 \sin^2 2\mu[\cos^2(\theta/2)/\cos\theta]^2 \times \left\{(3/U^3)\,(4\sin U - U\cos U - 3\mathrm{Si}U)\right\}^2 \quad (1)$$

$$R_{V_v} = \frac{16\pi^4}{\lambda_o^4}\left(\frac{4}{3}\pi R_s^3\right)^2 \cos^2\rho_1\,(3/U^3)^2 \left\{(\alpha_t - \alpha_s)\,(2\sin U - U\cos U - \mathrm{Si}\,U) + (\alpha_r - \alpha_s)\,(\mathrm{Si}\,U - \sin U) + (\alpha_r - \alpha_t)\,[\cos^2(\theta/2)/\cos\theta]\cos^2\mu\,(4\sin U - U\cos U - 3\,\mathrm{Si}\,U)\right\}^2 \quad (2)$$

where R is the scattering power measured in units of the Rayleigh ratio

$$R = I_s r^2/I_o V \quad (3)$$

where I_s is the scattered intensity measured with a detector at distance r from the sample, I_o is the incident intensity and V is the scattering volume. The subscript V_v designates vertically polarized incident radiation observed through a vertically oriented analyzer (Fig. 2) while H_v refers to a horizontally oriented analyzer. The wavelength of light in vacuum is λ_o and V_s is the spherulite volume. The scattering angles, θ and μ, are defined in Fig. 2. The angles ρ_1 and ρ_2 are defined by

$$\cos\rho_1 = \frac{\cos\theta}{(\cos^2\theta + \sin^2\theta\cos^2\mu)^{1/2}} \quad (4)$$

*Supported in part by grants from the Materials Research Laboratory, Univ. of Mass., the National Science Foundation, the Army Research Office (Durham) and the Petroleum Research Fund of the American Chemical Society.

ϕ To whom correspondence should be sent.
+ Present address: Monsanto Co., Birchem Bend Research Labs., Springfield, MA.
† Present address: Asahi Chemical Industry Co., Ltd., Fuji City, Shizuoka, Japan
o Present address: Raychem Corp., Menlo Park, California.

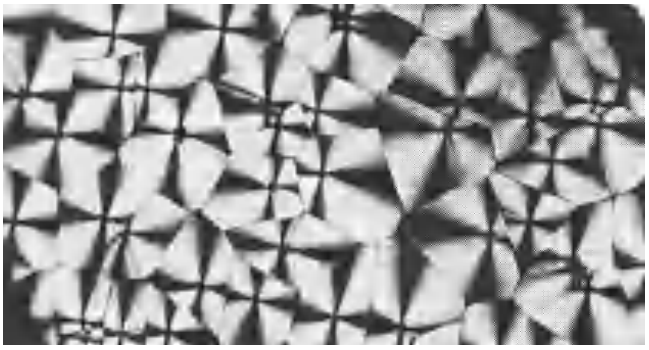

Fig. 1 An array of polyethylene spherulites as viewed between crossed polars in a microscope (from Ref. 24, Fig. 1).

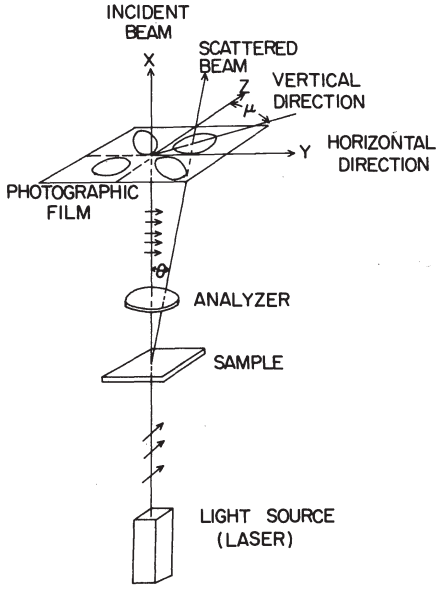

Fig. 2 The scattering angles and the polarization directions (from Ref. 45, Fig. 17).

$$\cos \rho_2 = \frac{\cos \theta}{(\cos^2\theta + \sin^2\theta \sin^2\mu)^{1/2}} \tag{5}$$

The reduced variable U is defined by

$$U = 4\pi(R_s/\lambda) \sin (\theta/2) \tag{6}$$

where λ is the wavelength of light in the medium (λ_o/n, where n is the refractive index). The angle θ should also be measured in the medium. The sine integral is defined by

$$\text{Si } U = \int_0^u (\sin x/x)\, dx \tag{7}$$

The theoretical H_v scattering pattern is shown in Fig. 3a where it is compared with the experimental pattern in Fig. 3b for a polyethylene film. Significant features of the patterns are intensity maxima at odd multiples of the azimuthal angle $\mu = 45^o$ and at a value of θ dependent upon the size of the spherulite. This maximum occurs at a value of U = 4.1 so that Eq. 6 gives.

$$4\pi(R_s/\lambda) \sin (\theta_{max}/2) = 4.1 \tag{8}$$

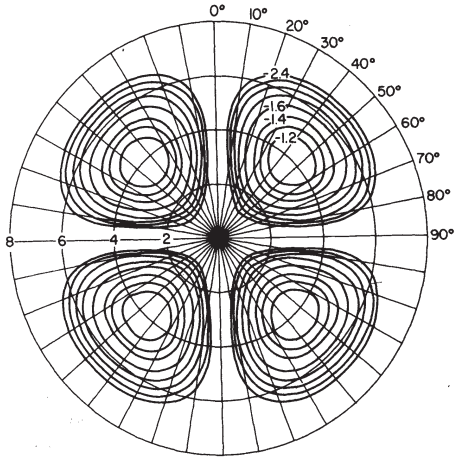

(a)

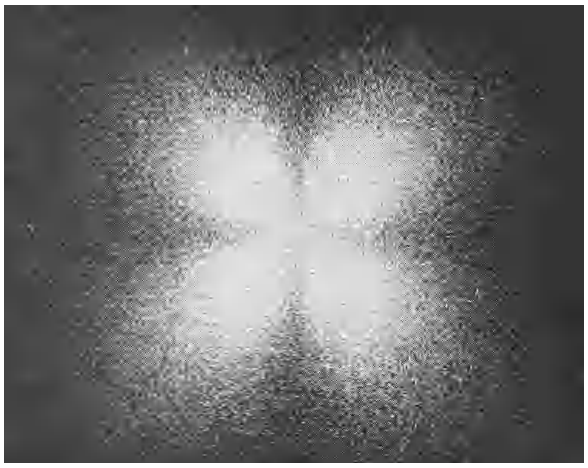

(b)

Fig. 3 A comparison of (a) theoretical and (b) experimental H_v scattering patterns.

This provides a convenient means for measuring changes in spherulite size, for example during the course of polymer crystallization. The change in spherulite size is evident from the series of H_v photographs of Fig. 4 obtained during the isothermal crystallization of polyethylene terephthalate (PET) from the melt at 120°C. Various automatic devices have been described[6-8] for following these changes and extensive use has been made[6] in following the kinetics of spherulite growth.

Similar equations have been obtained for two dimensional spherulites[9]. The effect of tilting of optic axes with respect to the spherulite radius and rotation of the optic axes about the radius has been explored, both in two[9] and three dimensions[10]. The effect of spherulite deformation in two[9] and three dimensions[11,12] has been calculated and has been used as a means for the study of spherulite deformation under both static[9] and dynamic[13,14] conditions.

RECENT PROGRESS

While photographic scattering studies give results that are in qualitative agreement with theory, more quantitative comparisons of scattered intensities with the predictions indicate the need for theoretical refinement. Quantitative measurements of the variation of scattered intensity with angle may be made with high resolution photometers[15,16] or else by using an optical multichannel analyzer[8]. Such intensity data must be corrected for refraction at sample interfaces as well as for multiple scattering[3]. The earlier multiple scattering corrections[3] were shown to be an overestimate and a better theory has been described[17,18]. These correction factors can be very significant and may often result in a several hundred percent modification of intensities.

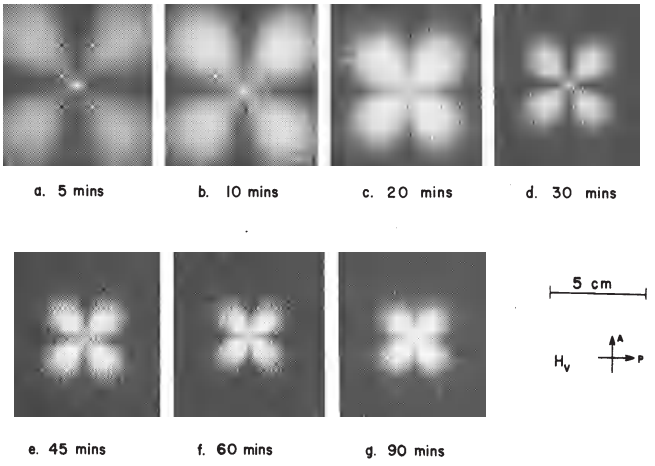

Fig. 4 The change in the H_v scattering patterns accompanying the isothermal crystallization of polyethylene terephthalate from the melt at 120°C. (from Ref. 24, Fig. 4).

A quantitative comparison of the theoretically calculated intensity with the experimentally measured leads to two important differences: (1) The theoretical intensity is zero at $\theta=0^0$ and falls off quite rapidly with increasing θ at angles greater than that of the maximum intensity, whereas the experimental intensity is finite at $\theta=0$ and is much greater than the theoretical prediction at large θ (Fig. 5)[19]. (2) The theory predicts that the H_v intensity should be zero at $\mu=0^0$ and 90^0 whereas finite intensities are found experimentally[20]. The differences are attributed to what has been referred to as external and internal disorder.

The external disorder is associated with phenomena related to difference in the configuration of the spherulitic boundary from the assumptions of the simple model. Such deviations arise from (1) incomplete spherulite development, (2) spherulite truncation resulting from impingement and (3) distribution of spherulite sizes. The vanishing of intensity at $\theta=0^0$ and $\mu=0^0$ and 45^0 is a consequence of spherical symmetry. Any irregularity of the shape of the spherulite may result in incomplete cancellation of scattered rays from complementary parts of the spherulite. Spherulites develop from rod-like nuclei and evolve through a sheaf-like stage. The accompanying evolution of the scattering patterns was described by Picot[21], Misra[22] and Stein and leads to the expected excess scattering at $\theta=0^0$ and $\mu=0^0$ and 90^0.

Another type of disorder arises from the fact that volume filling spherulites are not spheres but are truncated and meet at boundaries, forming polygonal shaped objects as seen in Fig. 1. Two-dimensional calculations of the scattering arising from such truncations, have been carried out[23]. For such systems, since there are no complete spherulites, the meaning of the spherulite radius becomes lost and this is replaced by a quantity $\bar{a}$ describing the average distance from the center of the spherulite to its boundary. The degree of truncation is described by a truncation parameter defined as

$$\sigma^2 = \overline{(a_i - \bar{a})^2} \tag{9}$$

This parameter is zero for a non-truncated spherulite. Its value was estimated from measurements on photomicrographs of spherulites as well as by computer calculations, assuming random placement of nuclei. The latter gave a value of $\sigma^2/\bar{a}^2 = 0.18$. It should be noted that random placement of nuclei leads to a value of σ which is smaller than that arising from regular placement. The value of effective spherulite radius, calculated through Eq. 8 is related to $\bar{a}$ in a manner dependent upon σ[24]. The value of scattering intensity corresponding to a particular value of effective spherulite radius calculated using Eq. 1 must also be modified by a factor dependent upon σ[24].

For non-volume filling spherulites, the value of σ varies from zero for the volume fraction of spherulites, $\phi_s=0$, to σ_{max} as ϕ_s approaches unity[25].

A third type of external disorder is related to the distribution of spherulite size which is a consequence of their mechanism of nucleation and growth. By assuming that spherulites scatter independently, the scattering from a collection of spherulites was calculated[26,27] using

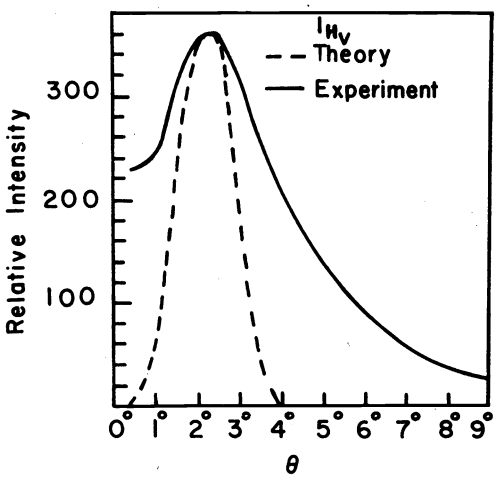

Fig. 5 A comparison of the experimental variation of scattered intensity from a polyethylene film with θ at $\mu = 45^0$ with the theoretical prediction (from Ref. 19, Fig. 1).

$$R = \sum_i N(R_i)\, R_1(R_i) \tag{10}$$

where $N(R_i)$ is the number of spherulites having radius R_i and $R_1(R_i)$ is the Rayleigh ratio for a single spherulite of this radius. By assuming various forms for $N(R_i)$, it was found that the angular distribution of scattering was broadened by an amount dependent upon the width of the distribution. However, this broadening was much smaller than that which was observed[19] suggesting that other factors to be presently discussed are the more important contributers to the broadening. For this reason, the determination of spherulite size distribution from the observed scattering intensity profile cannot be successful. Because of the much greater scattering power of larger spherulites, the effective spherulite size obtained using Eq. 8 from a distribution of sizes is heavily weighted with respect to the larger spherulites in the distribution.

Actually, different spherulites in a distribution will scatter coherently leading to interspherulitic interference effects. The resulting scattering pattern is obtained from the scattered amplitude given by[28]

$$E_s = \sum_i (E_1)_j\, e^{ik(\underset{\sim}{R}_j \cdot \underset{\sim}{s})} \tag{11}$$

where $(E_1)_j$ is the single spherulite amplitude for the j-th spherulite, $k = 2\pi/\lambda$, $\underset{\sim}{R}_j$ is the vector from an origin to the center of this spherulite. $\underset{\sim}{s}$ is the scattering vector $\underset{\sim}{s}_o - \underset{\sim}{s}_i$ where $\underset{\sim}{s}_o$ and $\underset{\sim}{s}_i$ are unit vectors along the incident and scattered rays. For small arrays of spherulites, this leads to a modulation of the pattern corresponding to their arrangement, while for a large array of randomly arranged spherulites, the result is like that of a single spherulite but containing an internal speckle structure of fineness dependent upon the number of spherulites in the field of view[29].

The internal disorder is related to the coarseness of the internal spherulitic structure. Electron micrographs of spherulites reveal that the lamella of which they are composed are not precisely aligned along their radius but are branched and fluctuate in their orientation[30]. For this reason, the model of constant polarizabilities throughout the spherulite is an idealization, and it is more realistic to assume that the local polarizabilities and the direction of their optic axes may fluctuate with position within the spherulite. An early model for disordered spherulites was proposed by Stein, Wilson and Stidham[31] in which density fluctuations were permitted within an isotropic sphere. These were defined in terms of the parameters η^2, the mean-squared fluctuation in density, and a correlation distance, a_c, for a Debye-Bueche type[5] exponential correlation function

$$\gamma(r) = \exp(-r/a_c) \tag{12}$$

where $\gamma(r)$ defined by

$$\gamma(r) = \langle \eta(x)\, \eta(x + r) \rangle_r / \eta^2 \tag{13}$$

$\eta(x)$ is the fluctuation of density at position λ and $\eta(\lambda + r)$ and a position r separated from λ. The symbol $\langle\rangle_r$ designates an average taken over all values of x for pairs of scattering elements at a fixed separation of r. Thus a_c is a measure of the coarseness of the fluctuation. It was shown that the model leads to the prediction of excess scattering at large angles in an amount dependent upon the values of η^2 and a_c.

Keijzers, van Aartsen and Prins[32] attempted to account for the excess scattering by spherulites using a mixture theory in which the scattering was proposed to consist of a component arising from perfect spherulites and one arising from a medium consisting of anisotropic objects correlated in orientation as described by the theory of Stein and Wilson[33].

This theory was not realistic in that the disorder consists of deviations from spherulitic order rather than being random. An attempt to treat spherulitic disorder was made by Stein and Chu[34] who considered correlated deviations from perfect spherulitic order as described by correlation functions. Because of mathematical difficulties, only simple cases could be evaluated. Alternatively, the problem was treated using a computer simulation by Yoon and Stein[19] who represented orientation deviations on a two-dimensional spherulitic lattice. The disorder was described in terms of a parameter δ which measured the angular deviation in orientation that could occur between two adjacent lattice cells. Typical results for the variation of the relative H_v scattered intensity with reduced angle $w = kR_s \sin\theta$ are shown in Fig. 6 at $\mu = 45^0$ for various values of the disorder parameter for a spherulite having M = 100 (lattice cells per radius). It is evident that as δ increases, the intensity at the maximum decreases and the decrease in intensity with increasing w becomes more gradual. In fact, as shown in Fig. 7, by taking the ratio of intensity at two values of w (in this case w = 4 to w = 15), one may obtain a calibration curve which may be used to determine δ. From this disorder parameter, the intensity decrease arising from the disorder may be obtained as shown in Fig. 8.

In this manner, by applying both disorder and truncation corrections, it is possible to satisfactorily fit experimental data as shown in Fig. 9. It should be noted that the fit should be viewed with reservation in that it is a two-dimensional theory applied to three-dimensional data. While the extension of the theory to three dimensions is demanding on computer capability, some success in this direction has been reported[35].

As previously indicated, the effect of considering interspherulitic interference for a collection of spherulites is to modulate the intensity in a manner dependent upon their distribution. The effect of this modulation on the average intensity for a random distribution of spherulites was considered by Yoon and Stein[36] using a correlation function approach. This led to the result for H_v scattering that

$$R_{H_v} = \frac{64}{3}\frac{\pi^5}{\lambda_o^4}\,\phi_s \cos^2\rho_2\,(\alpha_r - \alpha_t)^2\,R_s^3\,[\cos^2(\theta/2)/\cos\theta]^2$$
$$\times \sin^2 2\mu\,\left\{(3/U^3)\,(4\sin U - U\cos U - 3\,\mathrm{Si}\,U)\right\}^2$$
$$\times\,[\kappa(\theta,\mu)\,F(\theta,\mu)]^{-1} \qquad (14)$$

where $\kappa(\theta,\mu)$ is the correction factor for multiple scattering and $F(\theta,\mu)$ is that for disorder and truncation. It is noted that the scattered intensity varies linearly with ϕ_s, the volume fraction of spherulites. In addition the intensity depends upon the spherulite radius and the anisotropy, $(\alpha_r - \alpha_t)$ of the spherulite. This equation provides the means by which the absolute value of scattered intensity may be followed.

The anisotropy of a spherulite is a consequence of the orientation of its crystalline and amorphous components and may be given by

$$(\alpha_r - \alpha_t) = \phi_{cs}\,(\alpha_1 - \alpha_2)_c f_{c,s} + (1 - \phi_{cs})\,(\alpha_1 - \alpha_2)_{am} f_{c,am} + (\alpha_r - \alpha_t)_f \qquad (15)$$

where ϕ_{cs} is the volume fraction crystallinity of the spherulite, $(\alpha_1 - \alpha_2)_c$ and $(\alpha_1 - \alpha_2)_{am}$ are the intrinsic anisotropies of the crystalline and amorphous regions and $f_{c,s}$ and $f_{am,s}$ are the orientation functions for the optic axes of these regions with respect to the spherulite radius. The form anisotropy is $(\alpha_r - \alpha_t)_f$. The value of ϕ_{cs} is related to the crystallinity of the sample by

$$\phi_c = \phi_{cs}\,\phi_s + \phi_{cm}(1 - \phi_s) \qquad (16)$$

where ϕ_{cm} is the volume fraction crystallinity of the medium (outside the spherulites).

The value of $(\alpha_r - \alpha_t)_c$ may be calculated from the crystalline birefringence using the differential Lorenz-Lorentz equation

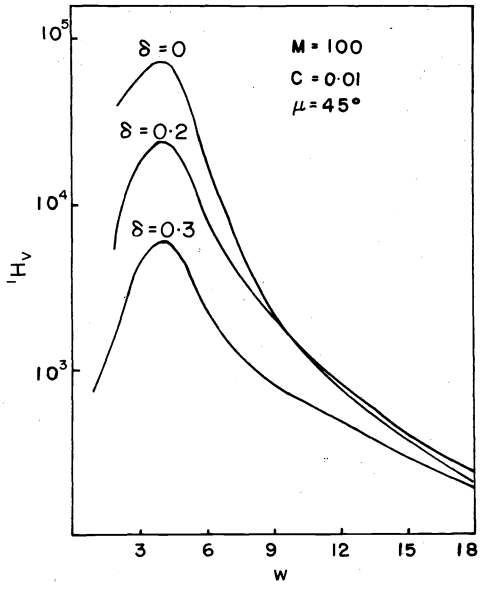

Fig. 6 The variation of relative H_V scattered intensity with w for various values of the disorder parameter (from Ref. 19, Fig. 6).

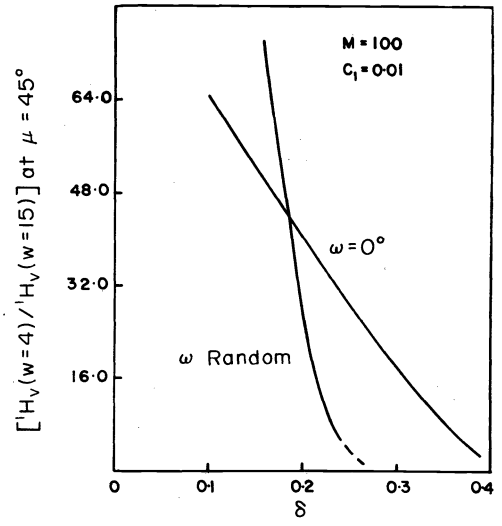

Fig. 7 The variation of the intensity ratio at two values of w with the disorder parameter. Two values of the optic axis twist angle ω are taken. One is where $\omega = 0^0$ (optic axis in plane of spherulite) and the other is for random twisting of the optic axis about the radius (from Ref. 19, Fig. 11).

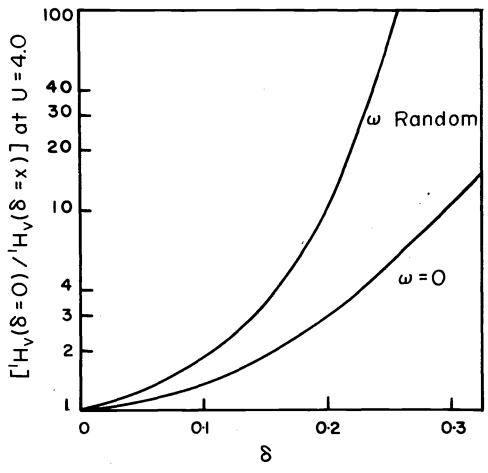

Fig. 8 The ratio of the H_v intensity for a perfect spherulite ($\delta = 0$) at $w = 4.0$, $\mu = 45^0$ to that of a disordered spherulite as a function of the disorder parameter. Curves for the same two cases of optic axis twist angle described in Fig. 7 are plotted (from Ref. 19, Fig. 13).

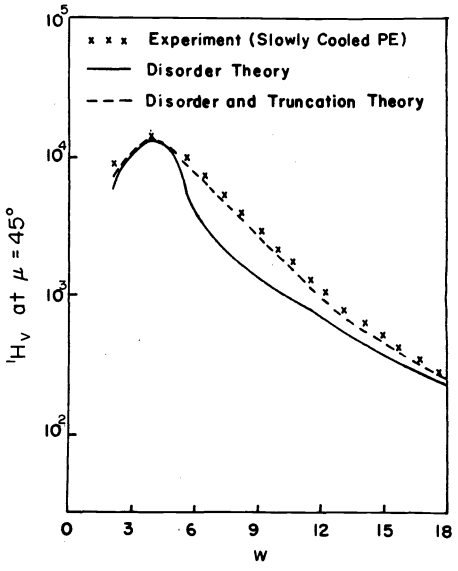

Fig. 9 A comparison of the experimental variation of the relative H_v intensity with w at $\mu = 45^0$ for a slowly cooled low density polyethylene sample with that theoretically predicted using disorder theory alone by applying a combination of disorder and truncation corrections (from Ref. 19, Fig. 14).

$$\Delta_c = \frac{2}{9}\pi \frac{(n_c^2 + 2)^2}{n_c} (\alpha_1 - \alpha_2)_c \qquad (17)$$

where n_c is the average refractive index of the crystals. For polyethylene, for example, $\Delta_c = 0.058$ from microscope measurements on isomorphic n-paraffin crystals[37]. While it is often assumed that the amorphous orientation in spherulites is negligible, recent calculations[38] suggest that it may make an appreciable contribution. The effect of form birefringence may be accessed by swelling the polymer with solvents of differing refractive index. While newer measurements are desirable, earlier work[39] has indicated that the effect of swelling on the intensity of scattering from unstretched polyethylene is not large.

It is usually assumed that all crystallization occurs within the spherulite so that $\phi_{c,m} = 0$. This may not be generally so. The intensity of V_v scattering, as may be seen from Eq. (2) is dependent upon α_s, the polarizability of the surroundings which is given by[19]

$$\alpha_s = \phi_s \left(\frac{\alpha_r + 2\alpha_t}{3} \right) + (1 - \phi_s)\alpha_m \qquad (18)$$

The polarizability of the medium, α_m is given by

$$\alpha_m = \phi_{c,m} \left(\frac{\alpha_1 + 2\alpha_2}{3}\right)_c + (1 - \phi_{c,m}) \left(\frac{\alpha_1 + 2\alpha_2}{3}\right)_{am} \quad (19)$$

Thus α_s and hence the intensity of the V_v scattering depend upon $\phi_{c,m}$. It is hoped that quantitative studies of this variation, perhaps following the photographic studies by Samuels[40] will clarify this situation.

If one assumes that $f_{am,s} = 0$, $\phi_{c,m} = 0$ and $(\alpha_1 - \alpha_2)_f = 0$ then Eqs. (15) and (16) give

$$(\alpha_r - \alpha_t) = \phi_c(\alpha_1 - \alpha_2)_c f_{c,s}/\phi_s \quad (20)$$

For a perfect spherulite $f_{c,s} = 1$ (or - 1/2). Deviations from these values are a consequence of imperfections, the effect of which is included in the factor $F(\theta,\mu)$ of Eq. (14) so that its inclusion in this term is redundant.

It is evident that substitution of Eq. (20) into Eq. (14) permits a calculation of the absolute value of R_{H_v} in terms of R_s, ϕ_c and ϕ_s. For volume filling spherulites, $\phi_s = 1$ in which case light scattering permits the calculation of the degree of crystallinity.

Similar but more complicated equations have been obtained for V_v scattering which account for the observation that the intensity passes through a maximum in the course of crystallization, and that the form of the patterns depends upon ϕ_s[19]. Thus there is the possibility that the simultaneous observation of R_{H_v} and R_{V_v} during the course of crystallization will permit a thorough characterization of the crystallization process. This is facilitated by the use of real-time devices such as the OMA.

EXPERIMENTAL APPLICATIONS

The use of these principles for the analysis of light scattering have so far been made in two studies: the crystallization of polyethylene terephthalate (PET) initiated by A. Misra[22,41] and continued by T. Yuasa[42] and the crystallization of blends of poly-ε-caprolactone (PCL) and polyvinyl chloride (PVC) by F. Khambatta[43].

Samples of PET were heated between aluminum foil to above their melting point and then rapidly cooled to a crystallizing temperature of 110°C. for varying periods of time, after which they were quenched to room temperature where crystallization stopped. H_v light scattering photographs were obtained as shown in Fig. 4. Scans of the variation of the relative scattered intensity with scattering angle, θ at $\mu = 45^0$ are shown in Fig. 10. These were obtained using the dynamic light scattering apparatus which has been described previously[44]. The shift of the scattering maximum toward lower angles was used to obtain the variation of spherulite radius with crystallization time as shown in Fig. 11. As has been previously observed[6], the radius increases linearly with time until it asymptotically approaches a limiting value when the spherulites become volume filling. This behavior is consistent with that predicted by model calculations[25].

The intensity at the H_v maximum increases greatly with crystallization time as shown in Fig. 12. The reason for this is three fold, as described by Eqs. 1 or 14: There is an increase in (a) the radius of the spherulites, (b) their number or (c) their anisotropy. Quantitative comparison of the results of Figs. 11 and 12 demonstrates that the increase in R_s is insufficient to account for the intensity increase. If one assumes that the spherulite anisotropy remains constant with time during crystallization ($\phi_{c,s}$ constant or no secondary crystallization), then Eqs. 14 and 20 may be used to calculate ϕ_s. If ϕ_c is determined by an independent measurement such as density, giving the results shown in Fig. 13, then ϕ_s may be obtained even if ϕ_{cs} changes.

This has been done for this sample of PET using H_v data corrected for multiple scattering and disorder (using the two-dimensional disorder theory) and leads to the results shown in Fig. 14. It is evident that there is an expected increase of volume fraction crystallinity with time. This may be related to the change in N_s, the number of spherulites per cm^3 since

$$\phi_s = N_s (4/3\ \pi\ R_s^3) \quad (21)$$

Solving this for N_s leads to the unexpected result that N_s decreases with time. This is not likely in view of reasonable crystallization mechanisms and it is thought that the result may be an artifact arising from the inadequacy of the two-dimensional disorder theory or perhaps from failure of the assumptions regarding the neglect of $\phi_{c,m}$. Further examination is in order, pending extension of the theory and analysis of V_v data.

For the analysis of PCL/PVC blends, samples were prepared by casting films from a mutual solvent, tetrahydrofuran, after which they were heated to above the melting point of the PCl

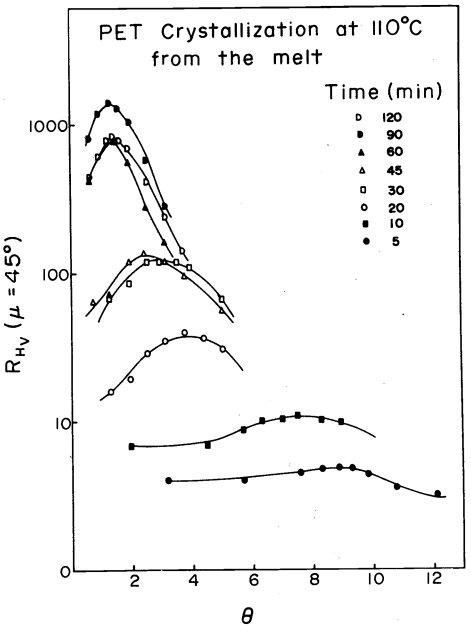

Fig. 10 The variation in the relative H_v light scattering intensity with angle θ at $\mu = 45^0$ for samples of PET crystallized at 110^0C. for varying periods of time (from Ref. 42, Fig. 14).

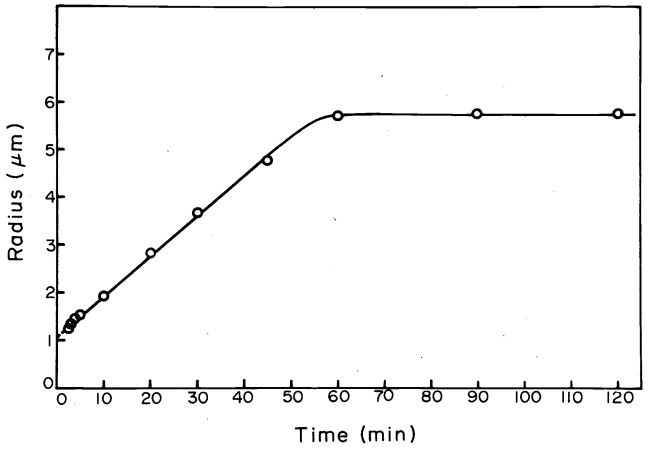

Fig. 11 The variation of spherulite radius with time for samples of PET crystallized at 110^0C. (from Ref. 42, Fig. 10).

and isothermally crystallized at 30^0C. Samples containing more than 50% PCL were observed microscopically to be composed of volume filling spherulites. This was confirmed by the observation that the linear crystallinity as measured by small-angle x-ray scattering agreed with the bulk crystallinity as measured by density or DSC[43,45] as shown in Fig. 15.

The variation of the spherulite size with composition was determined from the angular position of the H_v scattering maximum and is shown in Fig. 16 where it is seen to pass through a maximum. The variation of relative H_v intensity with scattering angle at $\mu = 45^0$ was measured with the photometric apparatus for the various blends and is plotted in Fig. 17. It is observed that there is an appreciable decrease in intensity of scattering with decreasing concentration of PCL. This is attributed to the decreasing anisotropy of the spherulite accompanying the decreasing sample crystallinity.

The only significant crystallinity is that of the PCL. Assuming that spherulites are volume filling and that the contribution of amorphous orientation and form anisotropy to the spherulite anisotropy are negligible, Eqs. (15) and (16) become

$$(\alpha_r - \alpha_t) = \phi_c(\alpha_1 - \alpha_2)_c f_{c,s} \tag{22}$$

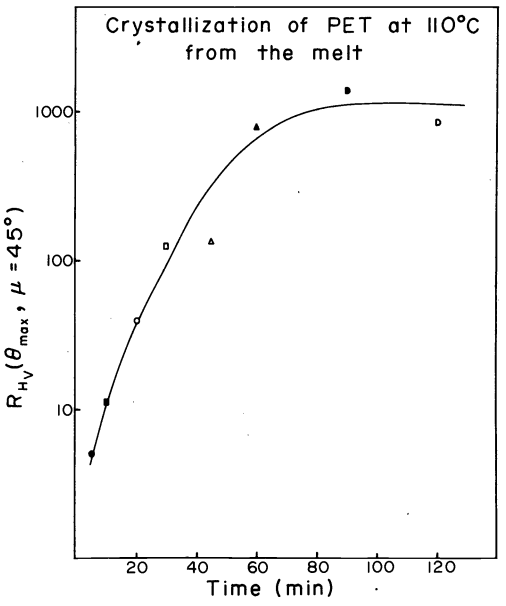

Fig. 12 The variation in the relative intensity at the H_V scattering maximum with crystallization time for PET at 110°C. (from Ref. 42, Fig. 15).

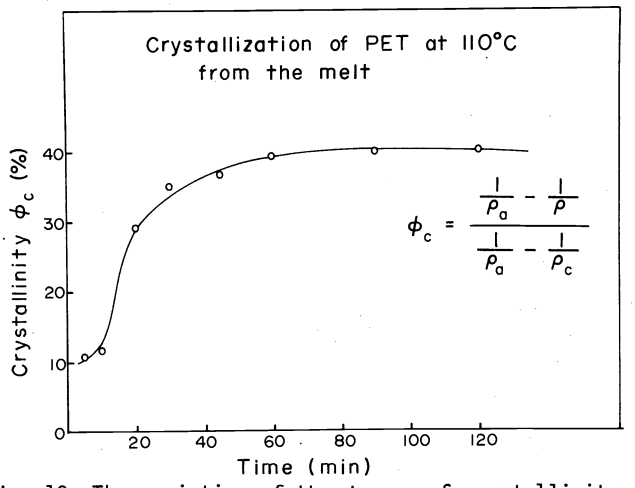

Fig. 13 The variation of the degree of crystallinity as determined from density with crystallization time for PET at 110°C. (from Ref. 42, Fig. 21).

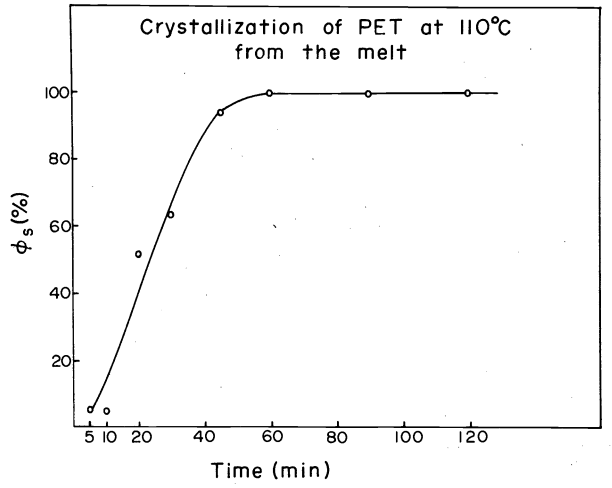

Fig. 14 The variation of calculated volume fraction of spherulites with crystallization time at 120°C. (from Ref. 42, Fig. 21).

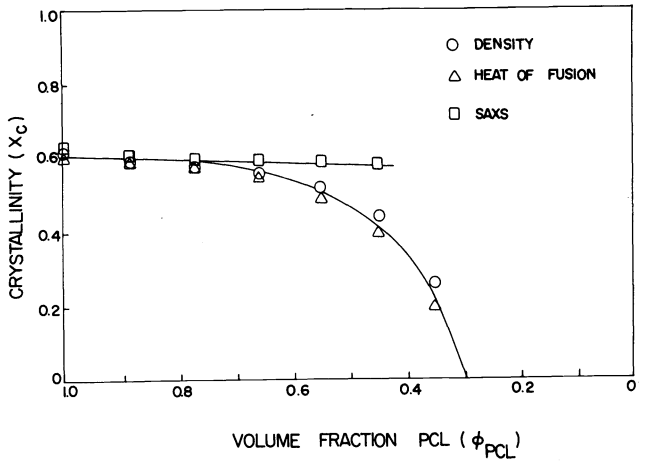

Fig. 15 The variation of the degree of crystallinity with composition of PCL/PVC blends as measured by density, DSC and small angle x-ray scattering (from Ref. 45, Fig. 1).

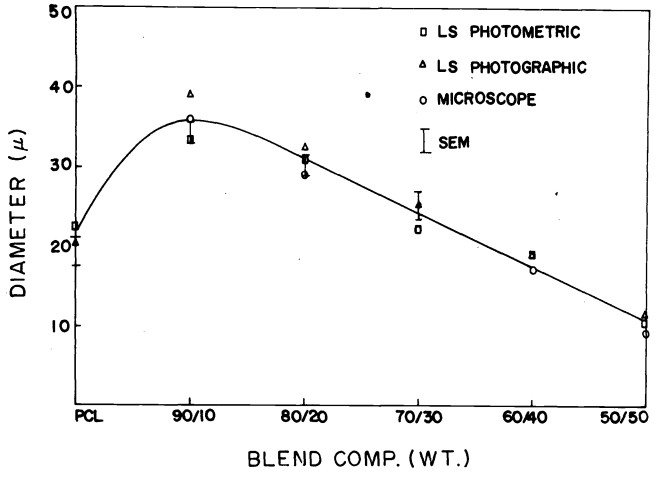

Fig. 16 The variation of spherulite size with composition of a PCL/PVC blend (from Ref. 45, Fig. 18).

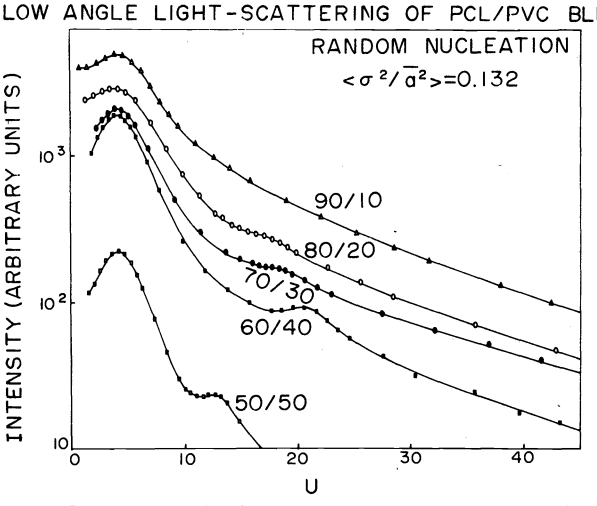

Fig. 17 The variation of relative H_v scattered intensity with scattering angle at $\mu = 45^0$ for the various blends (from Ref. 45, Fig. 19).

Thus by using measured degrees of crystallinity, evaluating $F(\theta,\mu)$ from the two-dimensional theory and realizing that it accounts for the effect of $f_{c,s}$, the variation of the relative H_v intensity with composition may be calculated and compared with the experimental result, as shown in Fig. 18. The comparison is reasonable except for high concentration of PCL where the films are very turbid so that the multiple scattering correction becomes suspect.

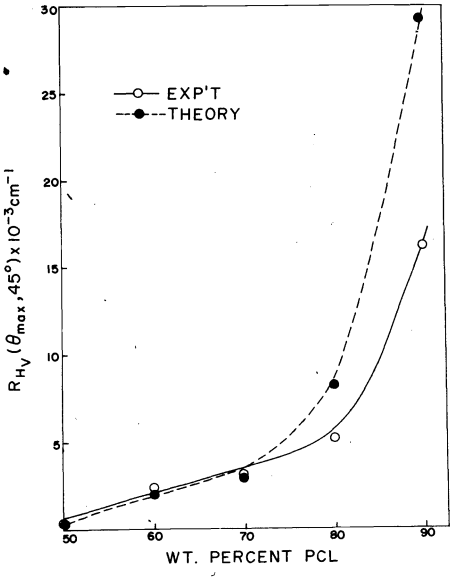

Fig. 18 A comparison of the calculated and measured variation of the relative intensity of the H_v scattering maximum with composition of a PCL/PVC blend (from Ref. 45, Fig. 20).

CONCLUSIONS

The photometric light scattering technique has been developed to the state where quantitative comparisons of measured scattered intensities with theoretically calculated values are useful for providing information about the crystallization process. The extension of the theory to three-dimensions, to the quantization of V_v data and to the further experimental examination of these and other systems are in order.

REFERENCES

1. R.S. Stein and M.B. Rhodes, J. Appl. Phys. 31 1873 (1960).
2. R.S. Stein in Structure and Properties of Polymer Films ed. by R.W. Lenz and R.S. Stein, Plenum Press, New York, 1973, p. 1.
3. R.S. Stein and J.J. Keane, J. Polym. Sci., 17 21 (1955).
4. J.J. Keane and R.S. Stein, J. Polym. Sci., 20 327 (1956).
5. P. Debye and A. Bueche, J. Appl. Phys. 30 518 (1949).
6. F. van Antwerpen and D.W. van Krevelen, J. Polym. Sci., Polym. Phys. Ed., 10 2409, 2423 (1972).
7. T. Pakula and Z. Soukup, J. Polym. Sci., Polym. Phys. Ed. 12 2437 (1974).
8. A. Wasiak, D. Peiffer and R.S. Stein, J. Polym. Sci., Polymer Letters Ed., 14 381 (1976).
9. S. Clough, J.J. van Aartsen, and R.S. Stein, J. Appl. Phys. 36 3072 (1965).
10. T. Hashimoto, Y. Murakami, Y. Okamori and H. Kawai, Polymer J. 6 554 (1974).
11. R. Samuels, J. Polym. Sci., C, 13, 37 (1966).
12. J.J. van Aartsen and R.S. Stein, J. Polym. Sci., A2, 9 295 (1971).
13. P.F. Erhardt and R.S. Stein, in High Speed Testing, Vol. IV, The Rheology of Solids (Appl. Polym. Symp. 5), Interscience, New York, 1967, p. 113.
14. P.F. Erhardt and R.S. Stein, J. Appl. Phys. 39, 4898 (1968).
15. R.S. Stein, F.H. Norris and A. Plaza, J. Polym. Sci. 24 455 (1957).
16. A.E.M. Keijzers, J.J. van Aartsen and W. Prins, J. Appl. Phys. 36 2874 (1965).
17. R.E. Prud'homme, L. Bourland, R.T. Natarajan and R.S. Stein, J. Polym. Sci., Polym. Phys. Ed. 12, 1955 (1974).
18. R. Natarajan, R.E. Prud'homme, L. Bourland and R.S. Stein, J. Polym. Sci., Polym. Phys. Ed. 14, 1541 (1976).
19. D.Y. Yoon and R.S. Stein, J. Polym. Sci., Polym. Phys. Ed., 12 763 (1974).
20. R.S. Stein, P.F. Erhardt, S.B. Clough and G. Adams, J. Appl. Phys. 37 3980 (1966).
21. C. Picot, R.S. Stein, M. Motegi and H. Kawai, J. Polym. Sci., A2, 8, 2115 (1970).
22. A. Misra and R.S. Stein, J. Polym. Sci., Polym. Phys. Ed. 11 109 (1973).
23. C. Picot and R.S. Stein, J. Polym. Sci., A2, 8, 2127 (1970).

24. R.E. Prud'homme and R.S. Stein, J. Polym. Sci., Polym. Phys. Ed. 11 1683 (1973).
25. A. Wasiak, S.D. Hong and R.S. Stein, in preparation.
26. M.B. Rhodes, P.R. Wilson, S.N. Stidham and R.S. Stein, Pure & Appl. Chem. 4 219 (1962).
27. T. Ishikawa and R.S. Stein, Polymer J., 8 369 (1976).
28. R.S. Stein and C. Picot, J. Polym. Sci., A2, 1955 (1970).
29. C. Picot, R.S. Stein, R.H. Marchessault, J. Borch and A. Sarko, Marcomolecules 4 467 (1971).
30. P. Geil, Polymer Single Crystals Interscience Publishers, New York, 1963, Chapt. IV.
31. R.S. Stein, P.R. Wilson and S.N. Stidham, J. Appl. Phys. 34 46 (1963).
32. A.E.M. Keijzers, J.J. van Aartsen and W. Prins, J. Am. Chem. Soc., 90 3167 (1968).
33. R.S. Stein and P.R. Wilson, J. Appl. Phys. 33 1914 (1962).
34. R.S. Stein and W. Chu, J. Polym. Sci., A2, 8 1137 (1970).
35. D.Y. Yoon and W. Chu, pvt. communication.
36. D.Y. Yoon and R.S. Stein, J. Polym. Sci., Polym. Phys. Ed. 12 735 (1974).
37. C.W. Bunn and R. de Daubeny, Trans. Faraday Soc. 50 1173 (1954).
38. V. Petraccone, I.C. Sanchez and R.S. Stein, J. Polym. Sci., Polym. Phys. Ed., 13 1991 (1975).
39. R.S. Stein in Growth and Perfection of Crystals, ed. by R.H. Doremus, B.W. Roberts and D. Turnbull, John Wiley & Sons, New York (1958).
40. R.J. Samuels, J. Polym. Sci., A2, 9, 2165 (1971).
41. A. Misra, Ph.D. Thesis, Univ. of Mass., Amherst, Mass., 1974.
42. T. Yuasa, MS Thesis, Univ. of Mass., Amherst, Mass., 1975.
43. F. Khambatta, Ph.D. Thesis, Univ. of Mass., Amherst, Mass., 1976.
44. T. Hashimoto, R.E. Prud'homme, D.A. Keedy and R.S. Stein, J. Polym. Sci., Polym. Phys. Ed. 11 693 (1973).
45. F. Khambatta, T. Russell, F. Warner and R.S. Stein, J. Polym. Sci., Polym. Phys. Ed., 14 1391 (1976).